

# microRNA-455-5p alleviates neuroinflammation in cerebral ischemia/reperfusion injury

<https://doi.org/10.4103/1673-5374.332154>

Date of submission: June 12, 2021

Date of decision: September 15, 2021

Date of acceptance: November 2, 2021

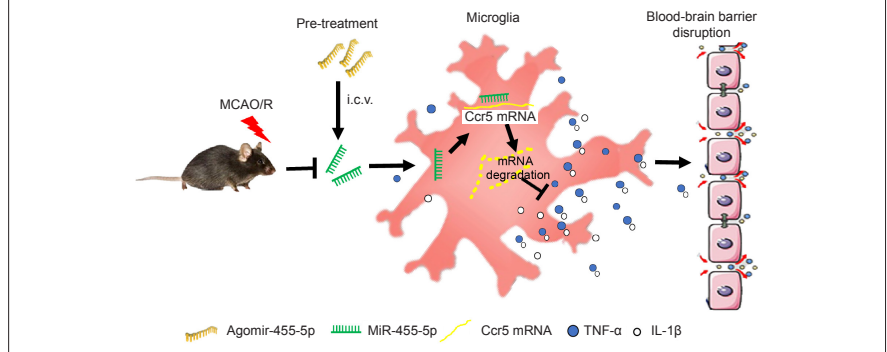
Date of web publication: January 7, 2022

## From the Contents

Introduction	1769
Materials and Methods	1770
Results	1771
Discussion	1774

Jian-Song Zhang<sup>1,2,#</sup>, Pin-Pin Hou<sup>1,#</sup>, Shuai Shao<sup>2,#</sup>, Anatol Manaenko<sup>3</sup>, Zhi-Peng Xiao<sup>2</sup>, Yan Chen<sup>4</sup>, Bing Zhao<sup>2</sup>, Feng Jia<sup>2</sup>, Xiao-Hua Zhang<sup>2</sup>, Qi-Yong Mei<sup>5,\*</sup>, Qin Hu<sup>1,2,\*</sup>

**Graphical Abstract** *microRNA-455-5p alleviates neuroinflammation through suppressing C-C chemokine receptor type 5 in MCAO mice*



## Abstract

Neuroinflammation is a major pathophysiological factor that results in the development of brain injury after cerebral ischemia/reperfusion. Downregulation of microRNA (miR)-455-5p after ischemic stroke has been considered a potential biomarker and therapeutic target for neuronal injury after ischemia. However, the role of miR-455-5p in the post-ischemia/reperfusion inflammatory response and the underlying mechanism have not been evaluated. In this study, mouse models of cerebral ischemia/reperfusion injury were established by transient occlusion of the middle cerebral artery for 1 hour followed by reperfusion. Agomir-455-5p, antagomir-455-5p, and their negative controls were injected intracerebroventricularly 2 hours before or 0 and 1 hour after middle cerebral artery occlusion (MCAO). The results showed that cerebral ischemia/reperfusion decreased miR-455-5p expression in the brain tissue and the peripheral blood. Agomir-455-5p pretreatment increased miR-455-5p expression in the brain tissue, reduced the cerebral infarct volume, and improved neurological function. Furthermore, primary cultured microglia were exposed to oxygen-glucose deprivation for 3 hours followed by 21 hours of reoxygenation to mimic cerebral ischemia/reperfusion. miR-455-5p reduced C-C chemokine receptor type 5 mRNA and protein levels, inhibited microglia activation, and reduced the production of the inflammatory factors tumor necrosis factor- $\alpha$  and interleukin-1 $\beta$ . These results suggest that miR-455-5p is a potential biomarker and therapeutic target for the treatment of cerebral ischemia/reperfusion injury and that it alleviates cerebral ischemia/reperfusion injury by inhibiting C-C chemokine receptor type 5 expression and reducing the neuroinflammatory response.

**Key Words:** agomir-455-5p; biomarker; blood-brain barrier; C-C chemokine receptor type 5; ischemia/reperfusion injury; ischemic stroke; microglia; microRNA-455-5p; neuroinflammation; pretreatment

## Introduction

Neuroinflammation is a major pathophysiological factor that contributes to the development of brain injury after cerebral ischemia/reperfusion (I/R). Within hours after I/R, cytokines and other proinflammatory mediators are released by injured cells, and circulating leukocytes are recruited and further infiltrate into the brain parenchyma (Jin et al., 2010; Buscemi et al., 2019; Xu et al.,

2020; Goebel et al., 2021). These effects aggravate the breakdown of the blood-brain barrier (BBB) and lead to further brain injury. Though hundreds of anti-inflammatory drugs have been successfully used in animal experiments, few are available to protect the human brain from I/R injury in the clinic (Zhou et al., 2018). Thus, novel therapeutic anti-inflammatory strategies are urgently needed.

MicroRNAs (miRNAs) are small non-coding RNAs that regulate

<sup>1</sup>Central Laboratory, Renji Hospital, Shanghai Jiao Tong University School of Medicine, Shanghai, China; <sup>2</sup>Department of Neurosurgery, Renji Hospital, Shanghai Jiao Tong University School of Medicine, Shanghai, China; <sup>3</sup>Department of Neurology, The First Affiliated Hospital of Chongqing Medical University, Chongqing, China; <sup>4</sup>Department of Medical Genetics, Shanghai Jiao Tong University School of Medicine, Shanghai, China; <sup>5</sup>Department of Neurosurgery, Changzheng Hospital, the Second Military Medical University, Shanghai, China

\*Correspondence to: Qi-Yong Mei, MD, PhD, meiqiyong@smmu.edu.cn; Qin Hu, MD, PhD, huqinle20010709@126.com.

<https://orcid.org/0000-0002-2270-8822> (Qin Hu)

#These authors contributed equally to this study.

**Funding:** This study was supported by the National Natural Science Foundation of China, Nos. 82071283 (to QH) and 81671130 (to QH); Medical Engineering Cross Research Foundation of Shanghai Jiao Tong University of China, No. YG2017MS83 (to QH); and from Shanghai Municipal Science and Technology Commission Medical Guidance Science and Technology Support Project of China, No. 19411968400 (to QYM).

**How to cite this article:** Zhang JS, Hou PP, Shao S, Manaenko A, Xiao ZP, Chen Y, Zhao B, Jia F, Zhang XH, Mei QY, Hu Q (2022) microRNA-455-5p alleviates neuroinflammation in cerebral ischemia/reperfusion injury. *Neural Regen Res* 17(8):1769-1775.

gene expression post-transcriptionally and are widely expressed in eukaryotic cells. Numerous miRNAs have been reported to promote or inhibit neuroinflammation by interfering with their target mRNAs (van Kralingen et al., 2019; Zuo et al., 2019). As a tumor-associated miRNA, miR-455-5p is characterized by its ability to suppress tumor metastasis (Liu et al., 2016; Hu et al., 2019, 2020). Recently, several studies have revealed that miR-455-5p attenuated inflammation by suppressing inflammation predicted targets, such as C-C chemokine receptor type 5 (CCR5) and suppressor of cytokine signaling 3 (Chen et al., 2019b; Xing et al., 2019). The level of miR-455-5p was downregulated after ischemic stroke and was suggested as a potential biomarker and therapeutic target for post-ischemic neuronal damage (He et al., 2016). However, the specific role of miR-455-5p and its mechanism have not been assessed yet. In the present study, we studied whether I/R affects the expression of miR-455-5p in mice and whether miR-455-5p is a potential I/R injury biomarker. Furthermore, we investigated the signaling pathway underlying the protective effect of miR-455-5p.

## Materials and Methods

### *In vivo experiments*

#### **Animals and experimental design**

All animal experiments were conducted in agreement with the regulations of the Animal Care and Use Committee of Shanghai Jiao Tong University School of Medicine, Shanghai, China (approval No. A-2018-004, approved on July 7, 2018). Because the estrogen level affects the pathophysiology of ischemic stroke (Koellhoffer and McCullough, 2013), specific-pathogen-free male C57BL/6 mice (20–25 g, 8–10 weeks old) were purchased from Shanghai Lingchang Biological Technology Limited Company (Shanghai, China; license No. SCSK [Hu] 2018-0003). A total of 261 mice were randomly divided into 10 groups: sham ( $n = 33$ ), I/R ( $n = 38$ ), pretreatment with miR-455-5p (Agomir + I/R,  $n = 39$ ) and its negative control (Agomir-NC + I/R,  $n = 44$ ), pretreatment with miR-455-5p antagonist (Antagomir + I/R,  $n = 39$ ) and its negative control (Antagomir-NC + I/R,  $n = 39$ ), miR-455-5p post-treatment (I/R-0h + Agomir,  $n = 7$ ; and I/R-1h + Agomir,  $n = 7$ ) and the corresponding negative control (I/R-0h + Agomir-NC,  $n = 7$ ; and I/R-1h + Agomir-NC,  $n = 8$ ). Detailed information about the animal assignments is provided in **Additional Figure 1** and **Additional Table 1**. The investigators were blinded to the group assignments during all outcome assessments.

#### **Cerebral I/R model**

To induce I/R injury, the middle cerebral artery was transiently occluded as previously described (Wang et al., 2020a). Briefly, the mice were anesthetized with isoflurane (4% induction concentration and 2% maintenance concentration; RWD Life Science, Shenzhen, China). The neck skin was cut along the midline, and the left common carotid artery, the internal carotid artery, and the external carotid artery were separated carefully. The left middle cerebral artery was blocked with a 6-0 nylon suture (702234PK5Re, Docol, Sharon, MA, USA). The body temperature (37°C) during the operation was controlled by a rectal sensor and heating pad (Harvard Apparatus, Holliston, MA, USA). Cerebral blood flow was monitored with a transcranial laser Doppler (moor VMS-LDF2, Moor Instruments, Axminster, UK). Eighty percent reduction in cerebral blood flow compared with the baseline was considered a successful middle cerebral artery occlusion (MCAO). Mice with regional cerebral blood flow during occlusion higher than 20% of the baseline were excluded. After 1 hour of occlusion, the suture was removed and the skin incision was closed. All the mice were housed separately with free access to food and water. Sham animals underwent the same surgical procedures without the MCAO.

#### **Intracerebroventricular injection**

MiR-455-4p mimic Agomir-455-5p, agomir-NC, MiR-455-4p antagonist antagomir-455-5p, and antagomir-NC (all provided by Sangon Biotech, Shanghai, China) were dissolved at a concentration of 0.08 nmol in 4  $\mu$ L of 0.01 M phosphate buffered saline (PBS) and were administered via intracerebroventricular injection 2 hours before or 0 and 1 hour after the MCAO (Zuo et al., 2019) (**Additional Figure 1** for the experimental design). Mice were fixed in a stereotaxic head frame (RWD Life Science). The head skin was cut along the midline and a burr hole was bored in the left side of the skull (1.0 mm lateral and 0.5 mm posterior to the bregma). Using a Hamilton syringe and a microinfusion pump (KDS 310, KD Scientific, Holliston, MA, USA), agomir-455-5p, agomir-NC, antagomir-455-5p, or antagomir-NC was infused into the left lateral ventricle at 0.2  $\mu$ L/min. After injection, the needle was left for an additional 5 minutes to

prevent possible leakage, then withdrawn slowly. The burr hole was sealed with bone wax and the incision was closed.

#### **Neurological behavior assessment**

The neurological deficits were assessed by the modified Garcia test by an experimenter (ZPX) blinded to the treatment procedures. The Garcia scores include six aspects: vibrissae touch, touch of trunk, climbing wall of wire cage, movements of forelimbs, spontaneous movements of all limbs, and spontaneous activity (Hu et al., 2017). The total score is 18 (healthy), and a lower score indicates serious deficits.

#### **2,3,5-Triphenyltetrazolium hydrochloride staining**

Fresh brain samples were collected 24 hours after MCAO and sectioned coronally at 1-mm intervals using a brain matrix (RWD Life Science). The slices were stained with 2,3,5-triphenyltetrazolium hydrochloride (MTT; Sigma-Aldrich, Darmstadt, Germany) for 20 minutes, and then fixed with 2% paraformaldehyde before being photographed. To reduce the interference of brain edema with the infarct volume, the infarction ratio was expressed as follows:  $1 - (\text{nonischemic ipsilateral hemisphere volume} / \text{whole contralateral hemisphere volume})$  (Zuo et al., 2019).

#### **Beam walking test**

Beam walking was used to assess fine motor coordination 1, 7 and 14 days after MCAO (Wang et al., 2020b). Mice were placed on a beam approximately 100 cm long and 0.8 cm wide. Foam pads were placed under the beam to protect mice from falling injury. The time to cross the beam was recorded by a detector with a timer and then analyzed. The maximum time allowed for the whole process was 2 minutes.

#### **Foot fault test**

The motor coordination of mice was tested by foot faults 1, 7 and 14 days after MCAO (Zuo et al., 2019). Mice were placed on a grid for 2 minutes to observe their movements. We monitored when the mouse's feet missed the grid and fell into the gap. The total number of mouse foot faults was recorded. The percentage of mouse foot faults was calculated and statistically analyzed.

#### **Brain water content**

Twenty-four hours after MCAO, the animals were anesthetized with isoflurane and decapitated. Brains were quickly extracted and separated into the left and right hemisphere and cerebellum. Samples were weighed before (wet weight) and after (dry weight) the brain tissue was placed in an oven at 105°C for 72 hours. The brain water content (%) was calculated as follows:  $100 - \text{dry weight} / \text{wet weight} \times 100$  (Zuo et al., 2019).

#### **Evaluation of BBB disruption (Evans blue assay)**

Two percent Evans blue (Sigma-Aldrich) was injected intraperitoneally (2 mL/kg of body weight) 22 hours after MCAO. The dye was allowed to circulate for 2 hours. After anesthesia with isoflurane, animals were perfused with ice-cold PBS via intracardial injection and euthanized. Brains were sectioned coronally at 1-mm intervals and photographed. Additionally, the ipsilateral hemisphere was collected and weighed. Then, 1 mL of PBS was added to the brain samples, which were homogenized, centrifuged at  $12,000 \times g$  for 20 minutes at 4°C, and the supernatants were collected. Half a milliliter of the supernatants was mixed with an equal volume of 100% trichloroacetic acid and incubated overnight at 4°C. On the next day, the samples were centrifuged and the supernatants were collected. The content of Evans blue in the ipsilateral hemisphere was calculated according to a standard curve (Zuo et al., 2019).

#### **In vitro microglia oxygen-glucose deprivation/reoxygenation model**

Primary microglia culture was performed as previously described (Chen et al., 2019a). Twenty-four neonatal 1–2-day-old C57BL/6J mice (Shanghai Lingchang Biological Technology Limited Company) were anesthetized with isoflurane and the brains were extracted rapidly. The cerebral cortices were dissected on ice and digested with 0.05% trypsin/ethylenediaminetetraacetic acid for 15 minutes at 37°C. Then, 10% fetal bovine serum in Dulbecco's modified Eagle's medium (Cat# 11965092, Thermo Fisher Scientific, Waltham, MA, USA) was added to stop the digestion. After centrifugation at  $300 \times g$  for 5 minutes, the cells were plated on poly-D-lysine-coated culture dishes and cultured with 10% fetal bovine serum in Dulbecco's modified Eagle's medium supplemented with B27 (Cat# 17504044, Thermo Fisher Scientific) at 37°C in a humidified 5% CO<sub>2</sub> atmosphere.

On day 11, microglial cells were collected by shaking the flasks at 5 × g for 2 hours, then cultured for 2 days. The purity of the microglial cultures was examined by immunostaining with a mouse monoclonal anti-ionized calcium-binding adapter molecule 1 (Iba1) antibody (1:200, Cat# ab15690, RRID:AB\_2224403, Abcam, Cambridge, UK) and Alexa 488-labeled goat anti-mouse IgG (Cat# ab150113, RRID:AB\_2576208, Abcam) and was determined to be > 97%.

An *in vitro* oxygen-glucose deprivation (OGD)/reoxygenation model was established as previously described (Ji et al., 2019). The medium of the microglial cells was replaced with glucose-free Dulbecco's modified Eagle's medium (Gibco, Cat#11966025) and transferred to a ProOx C21 hypoxia chamber (BioSpherix, Parish, NY, USA) containing 94% N<sub>2</sub>/5% CO<sub>2</sub>/1% O<sub>2</sub> for 3 hours. Reoxygenation was initiated by returning the cells to normal conditions, followed by addition of 100 nmol/mL agomiR-455-5p, antagomiR-455-5p, or their negative control to the medium.

#### Western blot assay

To study the role of miR-455-5p in the regulation of inflammation, the expression of CCR5, tumor necrosis factor-α (TNF-α), and interleukin-1β (IL-1β) were determined by western blotting at 24 hours after the OGD. The ipsilateral cortex samples were collected, homogenized with radio immunoprecipitation assay buffer (Cat# P0013B, Beyotime, Shanghai, China), and centrifuged. The supernatants were diluted with radio immunoprecipitation assay buffer and used for western blot assays (Zuo et al., 2019). After electrophoresis, proteins were transferred to polyvinylidene difluoride membranes. The membranes were blocked with 5% milk blocking buffer (nonfat milk diluted in Tris-buffered saline with Tween 20) for 1 hour. After several washes, the membranes were incubated with the following primary antibodies: rabbit polyclonal anti-CCR5 (1:1000, Cat# ab65850, RRID: AB\_1140936, Abcam), mouse monoclonal anti-TNF-α (1:1000, Cat# ab8348, RRID: AB\_306503, Abcam), rabbit polyclonal anti-IL-1β (1:1000, Cat# ab9722, RRID: AB\_308765, Abcam), or rabbit polyclonal anti-β-actin (1:1000, Cat# ab8227, RRID: AB\_2305186, Abcam) at 4°C overnight. Membranes were then washed with 1× Tris-buffered saline with Tween 20, incubated with secondary antibodies (goat anti-mouse IgG, 1: 2000, Cat# SA00001-1, RRID: AB\_2722565, Proteintech Group, Rosemont, IL, USA; goat anti-rabbit IgG, 1:2000, Cat# SA00001-2, RRID: AB\_2722564, Proteintech Group) for about 3 hours at room temperature, and exposed to a chemiluminescence detection system (FC12, Odyssey, Lincoln, NE, USA). For quantification, the optical density values of CCR5, TNF-α, and IL-1β, which were determined by ImageJ version 6.0 (National Institutes of Health, Bethesda, MD, USA), were normalized to β-actin.

#### Real-time polymerase chain reaction

To investigate the level of miR-455-5p in the brain tissue and the peripheral blood, RNA from the ipsilateral cortex and peripheral blood was extracted 24 hours after MCAO with Trizol (B511311, Sangon Biotech, Shanghai, China). PrimeScript™ RT reagent Kit with gDNA Eraser (RR047Q, Takara, Beijing, China) was used for reverse transcription. The following primers were used (Sangon Biotech, Shanghai, China): 18S, 5'-AGG AAT TCC CAG TAA GTG CG-3' (forward) and 5'-GCC TCA CTA AAC CAT CCA A-3' (reverse); *Ccr5*, 5'-TTT TCA AGG GTC AGT TCC GAC-3' (forward) and 5'-GGA AGA CCA TCA TGT TAC CCA C-3' (reverse); miR-455-5p, 5'-CGC GTA TGT GCC TTT GGA CT-3' (forward), 5'-AGT GCA GGG TCC GAG GTA TT-3' (reverse) and 5'-GTC GTA TCC AGT GCA GGG TCC GAG GTA TTC GCA CTG GAT ACG ACC GAT GT-3' (RT Primer); U6, 5'-CTC GCT TCG GCA GCA CA-3' (forward) and 5'-AAC GCT TCA CGA ATT TGC GT-3' (reverse). MIRNA First Strand cDNA Synthesis (Stem-loop Method) kit (B532453, Sangon Biotech, Shanghai, China) was used to detect miRNA. Real-time polymerase chain reaction (PCR) was performed with an ABI PRISM StepOnePlus System (Applied Biosystems, Thermo Fisher Scientific). The program parameters were 95°C for 5 minutes, followed by 40 cycles of 95°C for 30 seconds, 60°C for 30 seconds and 72°C for 30 seconds. U6 small nuclear RNA or 18S ribosomal RNA served as an internal reference. All the experiments were performed in triplicates and gene expression was analyzed using the 2<sup>-ΔΔCT</sup> method.

#### Luciferase assay

To identify whether *Ccr5* is a direct gene target of miR-455-5p, we cloned the 3' untranslated region (3'UTR) of the *Ccr5* gene with miR-455-5p and the respective mutant controls into the luciferase reporter plasmid PGL3 miReport vector (Cat# C8021, Promega, Madison, WI, USA). Human embryonic kidney 293T (HEK293T) cells (Cat# 12022001-1VL, RRID: CVCL\_0063, Merck, Burlington,

MA, USA) were co-transfected in 24-well plates with 0.5 μg of the 3'UTR luciferase reporter and 100 nM agomiR-455-5p, agomir-NC, antagomiR-455-5p, or antagomiR-NC, using 2.5 μL of RNAiMAX transfection reagent (Cat# 13778150, Thermo Fisher Scientific). Luciferase assays were performed with a Dual-Luciferase Reporter Assay System (Cat# E1910, Promega) 48 hours after transfection (Zuo et al., 2019). Normalization was calculated by the ratio of Renilla luciferase to firefly luciferase.

#### Immunofluorescence staining

To determine the cellular location of CCR5, double immunofluorescence staining of CCR5 with NeuN, Iba1, or Gfap was performed 24 hours after MCAO. The mice were intracardially perfused with PBS under anesthesia with isoflurane, and then fixed with 4% paraformaldehyde (Zuo et al., 2019). The brain samples were extracted, fixed for 24 hours with 4% paraformaldehyde, and dehydrated with 30% sucrose solution for 2 days. Coronal sections (10 μm) of the brain tissue were cut using a cryostat (CM1860UV, Leica Biosystems, Buffalo Grove, IL, USA). For permeabilization, sections were incubated for 30 minutes with 0.3% Triton X-100. After blocking with 10% bovine serum, the sections were incubated with the primary antibodies: rabbit anti-CCR5 antibody (1:200, Cat# ab65850, RRID: AB\_1140936, Abcam), mouse anti-NeuN antibody (1:200, Cat# ab104224, RRID: AB\_10711040, Abcam), mouse anti-Iba1 antibody (1:200, Cat# ab15690, RRID: AB\_2224403, Abcam), and mouse anti-Gfap antibody (1:200, Cat# 50-9892-82, RRID: AB\_2574408, Thermo Fisher Scientific) at 4°C overnight. After three 5-minute washes with PBS, the slices were incubated with the following secondary antibodies: Alexa 647-labeled donkey anti-rabbit IgG (1:500, Cat# ab150075, RRID: AB\_2752244, Abcam) or Alexa 488-labeled goat anti-mouse IgG (1:500, Cat# ab150113, RRID: AB\_2576208, Abcam) for 1 hour at room temperature. Imaging was performed on a laser scanning confocal microscope (Eclipse TE2000U, Nikon Instruments, Melville, NY, USA).

To study I/R-induced activation of microglia and astrocytes, their cell numbers and morphological alterations were analyzed. The number of Iba1- or Gfap-positive cells was counted as the average of three random fields at 400× magnification in each section, and three sections were analyzed per mouse. To determine the I/R-induced morphological alterations in microglia, the circularity index (CI, 4π[area]/[perimeter]<sup>2</sup>) and ramification index (RI, number of end branches/number of primary branches) were analyzed (33 cells from three sections per mouse) by Sholl analysis (ImageJ) as previously described (Otxoa-de-Amezaga et al., 2019).

#### Statistical analysis

No statistical methods were used to predetermine sample sizes; however, our sample sizes are similar to those reported in a previous study (Zuo et al., 2019). No animals or data points were excluded from the analysis. For statistical analyses, GraphPad Prism 6.0 software (GraphPad software, Inc., La Jolla, CA, USA) was used. Student's *t*-test was used to analyze the difference between two groups. For comparisons of multiple groups, one-way analysis of variance followed by Tukey's *post hoc* test was used. The data are presented as mean ± standard deviation (SD). Mortality was evaluated by Fisher's exact test. For data that did not meet the homogeneity of variance, non-parametric Kruskal-Wallis rank sum test was used. *P* < 0.05 was considered statistically significant.

## Results

### Pretreatment with agomiR-455-5p decreases infarct volume and improves neurological function in cerebral I/R mice

Twenty-four hours after the MCAO, I/R induced significant brain infarction and resulted in severe neurological deficits (*P* < 0.01, vs. sham group; **Figure 1A–C**). Treatment with agomiR-455-5p 2 hours before the MCAO effectively decreased the infarct volume (*P* < 0.01, vs. I/R group; **Figure 1A and B**) and ameliorated neurological deficits in cerebral I/R mice (*P* < 0.05, vs. I/R group; **Figure 1C**). However, no protective effects were observed when agomiR-455-5p was administered after reperfusion (**Additional Figure 2**). To further investigate the involvement of miR-455-5p in the development of post I/R injury, we silenced the expression of endogenous miR-455-5p by an antagomir. The results demonstrated that antagomiR-455-5p increased the infarct volume and aggravated I/R-induced neurological dysfunction (both *P* < 0.05, vs. I/R group; **Figure 1A–C**). Additionally, we conducted beam walking and foot fault tests to evaluate the long-term recovery of motor function. We found that animals in the Agomir + I/R group needed significantly less time to cross the beam at day 14, compared with the I/R group (*P* < 0.05,



vs. I/R group; **Figure 1D**). Furthermore, significant improvement of motor coordination and less misplacements were observed in the Agomir + I/R group in the foot fault test ( $P < 0.05$ , vs. I/R group; **Figure 1E**). In contrast, pretreatment with antagomiR-455-5p prolonged the beam crossing time ( $P < 0.05$ , vs. I/R group at day 14; **Figure 1D**) and increased the foot faults ( $P < 0.05$ , vs. I/R group at days 1, 7, and 14; **Figure 1E**). No statistically significant difference in mortality was observed between the I/R (16%) and Agomir + I/R groups (13%; **Additional Figure 3**). Moreover, administration of agomir-NC or antagomir-NC induced no significant difference in infarct volume and neurological deficits compared with the I/R group ( $P > 0.05$ ; **Figure 1**).

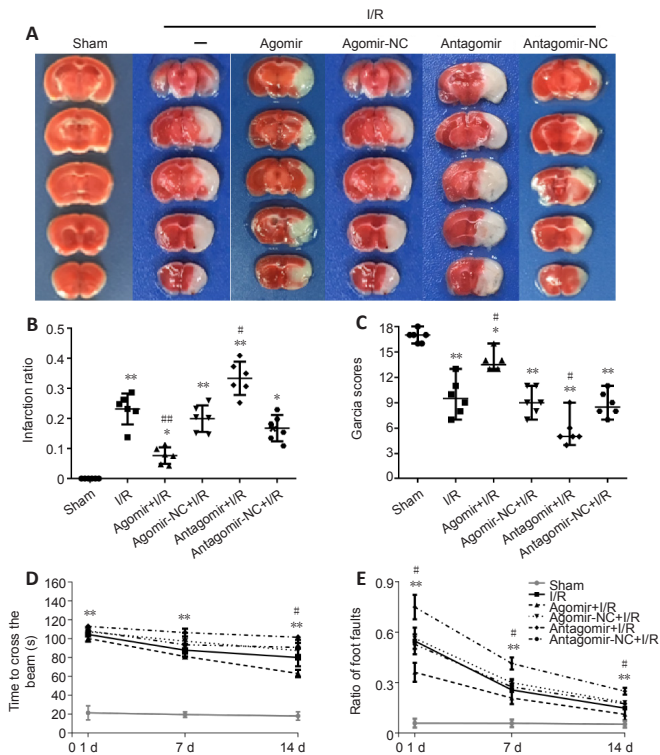


**Figure 1 | Pretreatment with agomiR-455-5p decreases the infarct volume and improves neurological function 24 hours after I/R.**

(A) Representative 2,3,5-triphenyltetrazolium hydrochloride-stained brain slices in mice of the following groups at 24 hours after surgery: Sham, I/R, I/R + pretreatment with agomiR-455-5p or antagomiR-455-5p, and I/R + the corresponding negative control. AgomiR-455-5p reduced the infarct volume; this effect was reversed by antagomiR-455-5p. (B) Quantitative results of the infarction ratio. (C) Garcia scores at 24 hours after I/R. (D) The beam crossing time in the beam walking test at 1, 7, and 14 days after I/R. The lower Garcia score or beam crossing time indicates serious deficits. (E) The results of the foot fault test at 1, 7, and 14 days after I/R. Data are presented as mean  $\pm$  SD ( $n = 6$  per group). Data of the infarction ratio and foot fault test were analyzed by one-way analysis of variance followed by Tukey's *post hoc* test, and the Garcia scores data were analyzed by non-parametric Kruskal-Wallis rank sum test. \* $P < 0.05$ , \*\* $P < 0.01$ , vs. sham group; # $P < 0.05$ , ## $P < 0.01$ , vs. I/R group. I/R: Ischemia/reperfusion; NC: negative control.

### Pretreatment with agomiR-455-5p protects BBB after cerebral I/R

Twenty-two hours after surgery, Evans blue stain was injected intraperitoneally. Animals were sacrificed 2 hours later, and brain samples were sectioned. Macroscopically, Evans blue was not found in the brain parenchyma of the sham-operated animals (**Figure 2A**). I/R induced the disruption of the BBB and significant staining was observed in the brain parenchyma (**Figure 2A**). Furthermore, we quantified the accumulation of Evans blue stain in the brain. Little Evans blue stain was detected in the nonischemic brain tissue, but the staining significantly increased after I/R ( $P < 0.01$ , vs. sham group; **Figure 2B**). Administration of agomiR-455-5p 2 hours before the MCAO effectively inhibited the extravasation of the Evans blue stain ( $P < 0.05$ , vs. I/R group), whereas pretreatment with antagomiR-455-5p aggravated the BBB disruption as evidenced by the increased content of Evans blue in the brain parenchyma ( $P < 0.05$ , vs. I/R group; **Figure 2A and B**). Additionally, to examine the treatment effect on brain edema formation we calculated the brain water content. AgomiR-455-5p significantly reduced the brain water content in the I/R mice

( $P < 0.01$ , vs. I/R group), whereas antagomiR-455-5p increased the brain water content ( $P < 0.01$ , vs. I/R group; **Figure 2C**). These results indicated that pretreatment with agomiR-455-5p protected the BBB integrity after I/R.

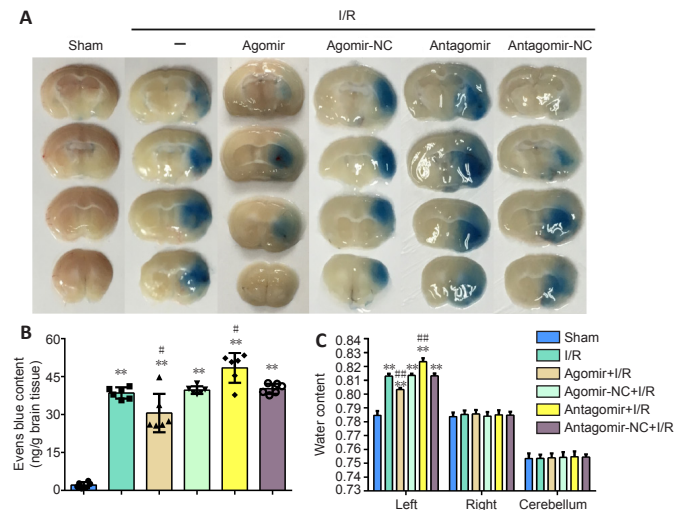


**Figure 2 | Pretreatment with agomiR-455-5p enhances the blood-brain barrier integrity at 24 hours after I/R.**

(A) Representative images of Evans blue extravasation in Sham, I/R, I/R + pretreatment with agomiR-455-5p or antagomiR-455-5p, and I/R + the corresponding negative control mice. AgomiR-455-5p inhibited the extravasation of Evans blue, whereas antagomiR-455-5p increased the extravasation. (B, C) Quantitative results of the content of Evans blue (B) and of the brain water content (C). Data are presented as mean  $\pm$  SD ( $n = 6$  per group). \*\* $P < 0.01$ , vs. sham group; # $P < 0.05$ , ## $P < 0.01$ , vs. I/R group (one-way analysis of variance followed by Tukey's *post hoc* test). I/R: Ischemia/reperfusion; NC: negative control.

### Ccr5 is a direct downstream target of miR-455-5p

Real-time PCR showed that I/R decreased the expression of miR-455-5p in the ipsilateral cortex ( $P < 0.05$ , vs. sham group; **Figure 3A**) and in the peripheral blood ( $P < 0.01$ , vs. sham group; **Additional Figure 4**) at 24 hours. As expected, agomiR-455-5p pretreatment increased the level of miR-455-5p in the brain ( $P < 0.01$ , vs. I/R group), whereas antagomiR-455-5p decreased the expression of miR-455-5p ( $P < 0.05$ , vs. I/R group; **Figure 3A**). The luciferase assay demonstrated that cotransfection of the miR-455-5p plasmid reduced the luciferase activity of the *Ccr5* 3'UTR reporter in HEK293T cells ( $P < 0.05$ , vs. agomir-NC + *Ccr5* 3'UTR group; **Figure 3B**). Consistently, pretreatment with agomiR-455-5p decreased the expression of *Ccr5* mRNA in the brain of cerebral I/R mice ( $P < 0.01$ , vs. I/R group; **Figure 3C**). Conversely, administration of antagomiR-455-5p increased the level of *Ccr5* mRNA ( $P < 0.05$ , vs. I/R group; **Figure 3C**). Additionally, the western blot results of CCR5 confirmed the mRNA results, i.e., agomiR-455-5p decreased the expression of CCR5 at the protein level ( $P < 0.05$ , vs. I/R group) and pretreatment with antagomiR-455-5p increased the CCR5 protein expression ( $P < 0.01$ , vs. I/R group; **Figure 3D and E**). Therefore, these results support the idea that *Ccr5* is a direct downstream target of miR-455-5p.

### AgomiR-455-5p prevents the activation of microglia 24 hours after cerebral I/R

Immunofluorescence was used to determine the location and expression of CCR5 in the brain tissue and examine the activation of microglia and astrocytes. CCR5 was highly expressed in neurons, astrocytes, and microglia 24 hours after I/R (**Figure 4**). Furthermore, the number of microglia and astrocytes was increased in the ischemic cortex compared with the sham animals (both  $P < 0.01$  vs. sham group; **Figure 5A and B**); however, pretreatment with agomiR-455-5p decreased the number of microglia but not of astrocytes ( $P < 0.01$  for microglia and  $P = 0.9602$  for astrocytes, vs. I/R group; **Figure 5A-C**). After ischemia, microglia in the ischemic cortex became activated and presented with an enlarged cell body (Circularity Index,  $P < 0.01$  vs. sham group; **Figure 5A and D**) and a reduced ramification (Ramification Index,  $P < 0.01$  vs. sham group; **Figure 5A and E**). Pretreatment with agomiR-455-5p attenuated the morphological alterations of microglia to a smaller cell body ( $P < 0.01$  vs. Agomir-NC + I/R group; **Figure 5A and D**) and an increased ramification ( $P < 0.01$  vs. Agomir-NC + I/R group; **Figure 5A and E**).

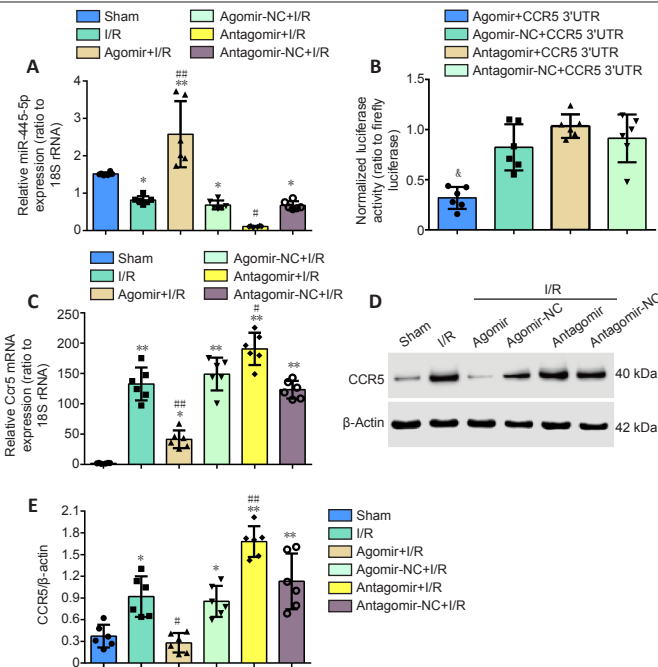


**Figure 3 | Ccr5 is a direct downstream target of miR-455-5p at 24 hours after the MCAO.**

(A) Relative expression of miR-455-5p in the ipsilateral cortex of Sham, I/R, I/R + pretreatment with agomiR-455-5p or antagomiR-455-5p, and I/R + the corresponding negative control mice at 24 hours. AgomiR-455-5p pretreatment increased the level of miR-455-5p, while antagomiR-455-5p inhibited the expression of miR-455-5p. (B) Result of the luciferase reporter assay. (C) Relative expression of Ccr5 mRNA at 24 hours after the MCAO. (D) Representative western blot bands of Ccr5. (E) Quantification of CCR5 protein expression at 24 hours after the MCAO. Data are presented as mean ± SD ( $n = 6$  per group). &P < 0.05, vs. Ccr5 3'UTR + agomiR-NC group; \*P < 0.05, \*\*P < 0.01, vs. sham group; #P < 0.05, ###P < 0.01, vs. I/R group (one-way analysis of variance followed by Tukey's *post hoc* test). Ccr5: C-C chemokine receptor type 5; I/R: ischemia/reperfusion; MCAO: middle cerebral artery occlusion; NC: negative control; rRNA: ribosomal RNA; snRNA: small nuclear RNA.

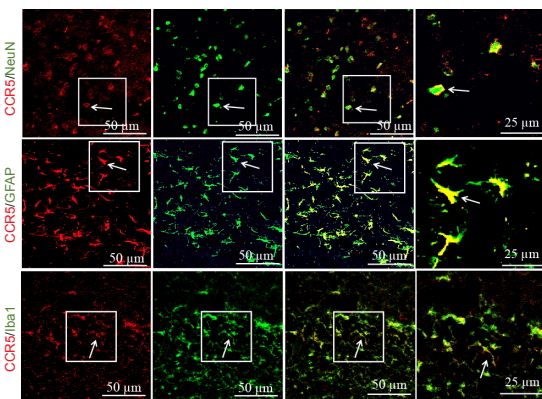


**Figure 4 | Representative immunofluorescent images of colocalization of CCR5 in neurons and glial cells in the ipsilateral cortex at 24 hours after I/R.**

CCR5 highly colocalized with NeuN (neuronal marker), Gfap (astrocytic marker), and Iba1 (microglial marker). Arrows indicated double stained cells. CCR5: red, Alexa Fluor® 647; NeuN: green, Alexa Fluor® 488; Gfap: green, Alexa Fluor® 488; Iba1: green, Alexa Fluor® 488. Scale bars: 50 μm in the three left columns, and 25 μm in the rightmost column. CCR5: C-C chemokine receptor type 5; GFAP: glial fibrillary acidic protein; Iba1: ionized calcium binding adaptor molecule 1; NeuN: neuronal nuclei.

**AgomiR-455-5p suppresses I/R-induced inflammation in primary cultured microglia and in cerebral I/R mice**

In primary cultured microglia subjected to OGD/reoxygenation, treatment with agomiR-455-5p significantly decreased the Ccr5 protein expression as well as the expression of proinflammatory factors TNF-α and IL-1β ( $P < 0.05$ , vs. AgomiR-NC group). In contrast, treatment with antagomiR-455-5p increased the expression of Ccr5, TNF-α, and IL-1β ( $P < 0.05$ , vs. AntagomiR-NC group, **Additional Figure 5**). In the cerebral I/R mice, I/R significantly increased the

production of proinflammatory mediators TNF-α and IL-1β in the ipsilateral cortex ( $P < 0.05$ , vs. sham group; **Figure 6**). However, pretreatment with agomiR-455-5p decreased the brain TNF-α and IL-1β production post I/R ( $P < 0.05$ , vs. I/R group; **Figure 6**). In contrast, pretreatment with antagomiR-455-5p enhanced the TNF-α ( $P < 0.01$ , vs. I/R group) and IL-1β production in the brain tissue ( $P < 0.05$ , vs. I/R group; **Figure 6**).

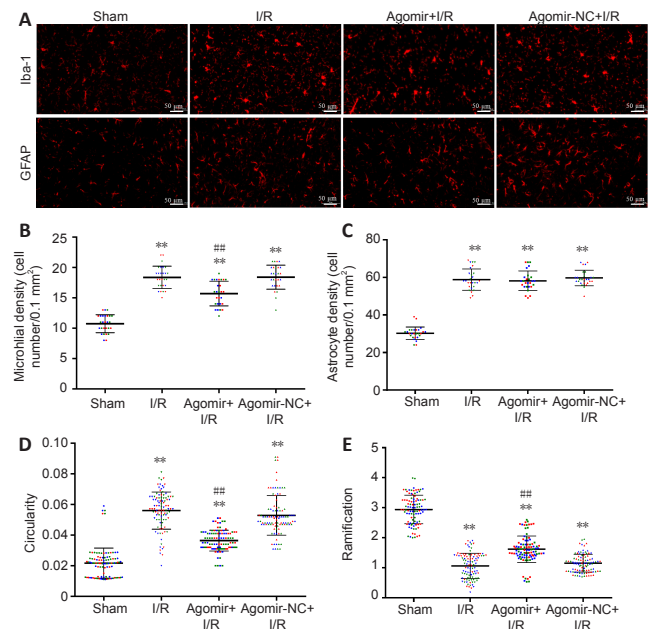


**Figure 5 | Pretreatment with agomiR-455-5p inhibits the activation of microglia at 24 hours after I/R injury in mice.**

(A) Representative images of Iba1 and Gfap in the ischemic cortex of Sham, I/R, I/R + pretreatment with agomiR-455-5p and its negative control animals 24 hours after I/R. Pretreatment with agomiR-455-5p decreased the number of microglia and attenuated the morphological alterations in microglia, resulting in a smaller cell body and increased ramification. Gfap: red, Alexa Fluor® 647; Iba1: red, Alexa Fluor® 647. Scale bars: 50 μm. (B, C) Quantitative results of the number of microglia and astrocytes in the ischemic cortex. (D, E) Quantitative results of the Circularity Index and Ramification Index of microglia. For each animal, 33 cells from three sections were analyzed; cells from different animals are represented by different colors. Data are presented as mean ± SD ( $n = 3$  mice per group). \*\*P < 0.01, vs. sham group; ###P < 0.01, vs. AgomiR-NC + I/R group (one-way analysis of variance followed by Tukey's *post hoc* test). GFAP: Glial fibrillary acidic protein; I/R: ischemia/reperfusion; Iba1: ionized calcium binding adaptor molecule 1; NC: negative control.

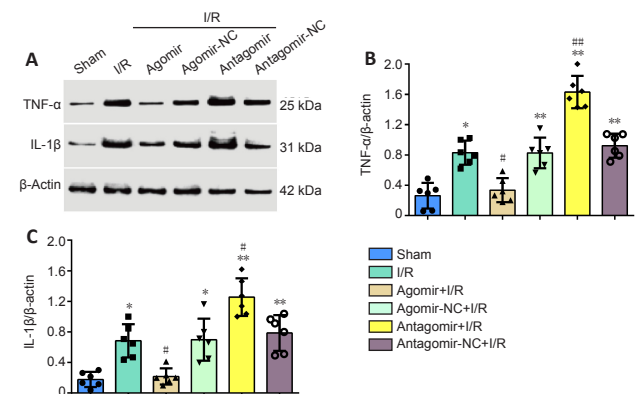


**Figure 6 | AgomiR-455-5p suppresses the inflammation in the ipsilateral cortex 24 hours after I/R.**

(A) Representative western blots of Tnf-α and IL-1β in Sham, I/R, I/R + pretreatment with agomiR-455-5p or antagomiR-455-5p, and I/R + the corresponding negative control animals. (B, C) Quantitative results of TNF-α and IL-1β expression in the ipsilateral cortex. Data are presented as mean ± SD ( $n = 6$  per group). \*P < 0.05, \*\*P < 0.01, vs. sham group; #P < 0.05, ###P < 0.01, vs. I/R group (one-way analysis of variance followed by Tukey's *post hoc* test). I/R: Ischemia/reperfusion; IL-1β: interleukin-1β; NC: negative control; TNF-α: tumor necrosis factor alpha.



## Discussion

Reperfusion is one of the most common factors that lead to aggravation of stroke-induced brain injury. In acute ischemic reperfusion, inflammation greatly contributes to neuronal cell death and BBB disruption; however, few anti-inflammation therapies have been proven to be beneficial in the clinical setting (Zhou et al., 2018). There is mounting evidence indicating that miRNAs are critically involved in the regulation of inflammation. Although it has been reported that as a member of the miR-455 family, miR-455-5p is critically involved in inflammation, its role in I/R-induced brain injury remained unclear (Torabi et al., 2019). Here, we demonstrated that I/R significantly downregulated miR-455-5p production in the brain tissue and in the peripheral blood in mice; however, augmentation of miR-455-5p expression with agomiR-455-5p effectively decreased the brain infarction, preserved the BBB integrity, and improved neurological function. Furthermore, pretreatment with agomiR-455-5p attenuated reperfusion-induced inflammation, resulting in decreased expression of inflammatory mediators Tnf- $\alpha$  and IL-1 $\beta$ . Most importantly, we verified that *Ccr5* is a direct gene target of miR-455-5p, which is negatively regulated by miR-455-5p. This downregulation was accompanied by suppression of the post-I/R inflammatory response. Stroke is unpredictable, hence medical intervention prior to stroke onset is mostly impossible. However, the number of patients undergoing cardiac surgery, e.g., coronary artery bypass grafting, is increasing every year with a high risk of perioperative stroke (Jovin et al., 2019). The surgery timeline enables administration of the drug at a defined time point, thus making pretreatment a promising therapeutic option. This approach is recommended by experts in the field (Salameh et al., 2016). Our study may provide a potential strategy for preventing the brain from ischemic injury and reducing perioperative complications.

Excessive and unresolved neuroinflammation is a major driver of brain damage after I/R (Jayaraj et al., 2019; Wang et al., 2020c). Ischemia leads to impaired energy metabolism immediately after insult, which eventually results in necrosis and apoptosis (Campbell et al., 2019). Furthermore, I/R leads to reactive oxygen species overproduction. The debris from injured cells and reactive oxygen species trigger an inflammatory response by recruiting systemic immune cells from the circulating blood as well as activating microglia and astrocytes. The released proinflammatory mediators from these cells increase the BBB permeability and induce neuronal cell death, leading to functional deficits. In the last decade, sufficient evidence has supported the hypothesis that miRNAs play an important role in regulating inflammatory signaling (Slota and Booth, 2019). As a member of the miR-455 family, miR-455-5p is involved in tumor suppression, and emerging evidence suggests that it negatively regulates inflammation (Torabi et al., 2019). Several master regulators of the inflammatory response, such as suppressor of cytokine signaling 3, Janus kinase 1, myeloid differentiation factor 88, and *Ccr5*, have been verified as miR-455-5p targets (Chen et al., 2019b; Torabi et al., 2019; Xing et al., 2019). MiR-455-5p represses these inflammatory signaling pathways, and consequently suppresses inflammation. In the central nervous system, miR-455-5p has been reported to be expressed in neurons, microglia, and astrocytes, and dysregulation of miR-455-5p has been demonstrated in numerous neurological diseases (Sierksma et al., 2018). Increased expression of miR-455-5p has been reported in rat dorsal root ganglion neurons after sciatic nerve transection (Strickland et al., 2011). MiR-455-5p is recognized as one of the miRNAs that are mostly affected by cerebral I/R injury and is linked to poor outcomes (He et al., 2016). A clinical study has established that miR-455-5p was greatly downregulated in the peripheral blood of ischemic stroke patients (He et al., 2016). In I/R mice, treatment with miR-455 mimics protected the brain against cerebral I/R injury-induced neuronal death by suppressing inflammation and decreasing the expression of Tnf receptor associated factor 3. Interestingly, our findings are consistent with these reports that I/R decreased the level of miR-455-5p in the brain tissue as well as in the peripheral blood. However, the decrease was followed by upregulated expression of the target gene *Ccr5*, along with increased production of the inflammatory mediators TNF- $\alpha$  and IL-1 $\beta$ .

The chemokine receptor, *Ccr5*, is a G-protein coupled receptor that is activated by  $\beta$ -chemokines and is widely implicated in increased neuroinflammation (Martin-Blondel et al., 2016). Previous studies have shown that *Ccr5* is constitutively expressed on macrophages and immune cells, as well as microglia and neurons, and it is upregulated after cerebral I/R (Sorace et al., 2011; Victoria et al., 2017;

Joy et al., 2019; Chen et al., 2020). In our study, a substantial increase in *Ccr5* expression was observed after I/R. Immunofluorescence double staining confirmed that it is highly expressed in neurons, glia, and microglia after I/R, and that the *Ccr5* level positively correlates with the inflammatory response. In cerebral I/R mice, the number of microglia and astrocytes in the ischemic cortex was significantly increased, and the microglia presented with an enlarged cell body and retracted processes. The morphology alterations of microglia observed here highly corresponded to their typical features reported previously. I/R induced microglia activation, accompanied with decreased miR-455-5p and increased *Ccr5* expression, leading to the release of proinflammatory mediators.

To date, downstream signaling pathways of *Ccr5* such as mitogen-activated protein kinase, signal transducer and activator of transcription 1, phosphatidylinositol-3 kinase, and cyclic AMP response element-binding protein have been discovered (Yang et al., 2010; Banerjee et al., 2011; Chien et al., 2018; Joy et al., 2019; Lan et al., 2019). As a coreceptor for the human immunodeficiency virus, *Ccr5* is responsible for cognitive deficits induced by impairing neuronal plasticity, learning, and memory in human immunodeficiency virus patients (Vangelista and Vento, 2017). In ischemic cerebrovascular disease, the role of *Ccr5* is discussed controversially. Patients with *Ccr5* D32 polymorphism presented increased risk of ischemic stroke (Joy et al., 2019). Sorace et al. (Sorace et al., 2010) have found that *Ccr5*-deficient mice displayed more serious neutrophil invasion and greater infarction compared with wild-type mice. However, several other studies have demonstrated that inhibition of *Ccr5* by its antagonist or genetic silencing led to a reduced infarct volume and a better neurological outcome in animal stroke models (Li et al., 2017; Victoria et al., 2017; Joy et al., 2019). AgomiR-455-5p reduced the luciferase activity of the plasmid containing the 3'UTR of the *Ccr5* gene, and inhibited the mRNA and protein expression of *Ccr5*, suggesting that miR-455-5p decreased *Ccr5* expression post-transcriptionally by binding to its 3'UTR. In primary cultured microglia, agomiR-455-5p reduced the protein expression of *Ccr5* and of the proinflammatory factors Tnf- $\alpha$  and IL-1 $\beta$ , 24 hours after OGD/reoxygenation. Accordingly, in cerebral I/R mice, pretreatment with agomiR-455-5p augmented the level of miR-455-5p and inhibited microglia activation, resulting in beneficial outcomes of reduced infarct size and improved neurological deficits. Given our findings, direct targeting of *Ccr5* may be the pathway responsible for the anti-inflammatory effect of miR-455-5p after I/R.

Our study has some limitations. We evaluated the anti-inflammatory properties of the treatment and its ability to protect the post-ischemic brain only in the acute stage of the disease, at 24 hours after the MCAO. However, the inflammatory response following ischemia evolves over a long time. Furthermore, while suppression of inflammation in the acute stage is beneficial, inflammation in the chronic stage of the disease is positively associated with brain repair (Jayaraj et al., 2019). Therefore, whether short-term protection, which was established in the current study, results in decreased brain inflammation at later time points and affects long-term brain recovery needs to be evaluated in future studies. Additionally, given that one miRNA can interact with hundreds of target genes, it is possible that other downstream targets of miR-455-5p are involved in the neuroprotection of miR-455-5p. Several small-molecule antagonists of *Ccr5*, including aplaviroc, vicriviroc, and maraviroc, have been reported with detrimental consequences of liver toxicity and resistance (Clotet, 2007). Compared with traditional small-molecule inhibitors, miRNAs have the advantages of targeting multiple genes simultaneously and being able to be easily chemically modified to improve their pharmacokinetics (Li and Rana, 2014). MiRNA-based therapeutics may be a viable option for inhibiting *Ccr5* function in the future, though challenges such as off-target effects, stability, and cell-specific targeting have not been resolved.

In conclusion, we demonstrated that miR-455-5p may serve as an I/R injury biomarker and that it diminished neuroinflammation by suppressing *Ccr5* expression, consequently alleviating I/R-induced injury. The miR-455-5p/*Ccr5* signaling pathway may provide a novel insight into ischemic stroke management, making it a promising therapeutic target.

**Author contributions:** Study design and manuscript draft: QH, QYM; animal model and behavioral tests: JSZ, SS; molecular studies: PPH, YC, BZ; data analysis: JSZ, SS, ZPX, FJ; manuscript revision: AM, XHZ. All authors read, revised, and approved the final manuscript.

**Conflicts of interest:** The authors declare that the research was conducted



in the absence of any commercial or financial relationships that could be construed as a potential conflict of interest.

**Availability of data and materials:** All data generated or analyzed during this study are included in this published article and its supplementary information files.

**Open access statement:** This is an open access journal, and articles are distributed under the terms of the Creative Commons AttributionNonCommercial-ShareAlike 4.0 License, which allows others to remix, tweak, and build upon the work non-commercially, as long as appropriate credit is given and the new creations are licensed under the identical terms.

©Article author(s) (unless otherwise stated in the text of the article) 2022. All rights reserved. No commercial use is permitted unless otherwise expressly granted.

**Open peer reviewer:** Claudia Espinosa-Garcia, Emory University, USA.

**Additional files:**

**Additional Figure 1:** Experimental design, animal groups classification and timeline.

**Additional Figure 2:** Administration of agomiR-455-5p at 0 and 1 hour after reperfusion had no protective effect on infarct volume and neurological deficits.

**Additional Figure 3:** The mortality of mice in the study.

**Additional Figure 4:** I/R reduces the level of miR-455-5p in the peripheral blood in cerebral I/R mice.

**Additional Figure 5:** AgomiR-455-5p inhibits the expression of CCR5 and pro-inflammatory factors TNF- $\alpha$  and IL-1 $\beta$  24 hours after OGD/reoxygenation (OGD/R), and antagomiR-455-5p reverses the effects.

**Additional Table 1:** Animal assignment in each group.

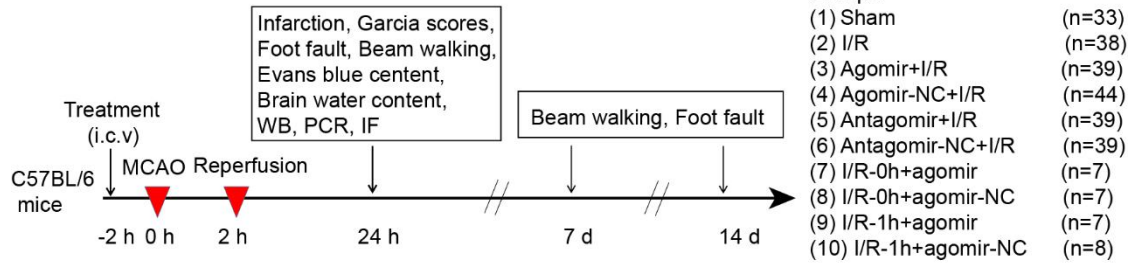
**Additional file 1:** Open peer review report 1.

## References

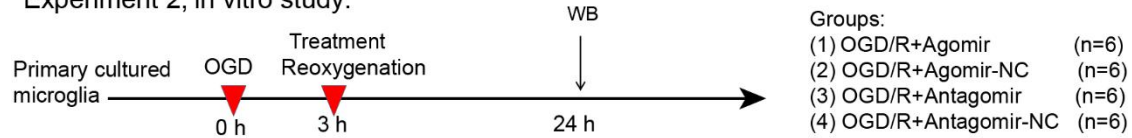
- Banerjee A, Pirrone V, Wigdahl B, Nonnemacher MR (2011) Transcriptional regulation of the chemokine co-receptor CCR5 by the cAMP/PKA/CREB pathway. *Biomed Pharmacother* 65:293-297.
- Buscemi L, Price M, Bezzi P, Hirt L (2019) Spatio-temporal overview of neuroinflammation in an experimental mouse stroke model. *Sci Rep* 9:507.
- Campbell BCV, De Silva DA, Macleod MR, Coutts SB, Schwamm LH, Davis SM, Donnan GA (2019) Ischaemic stroke. *Nat Rev Dis Primers* 5:70.
- Chen C, Chu SF, Ai QD, Zhang Z, Chen NH (2020) CKLF1/CCR5 axis is involved in neutrophils migration of rats with transient cerebral ischemia. *Int Immunopharmacol* 85:106577.
- Chen F, Weng Z, Xia Q, Cao C, Leak RK, Han L, Xiao J, Graham SH, Cao G (2019a) Intracerebroventricular delivery of recombinant namp1 deters inflammation and protects against cerebral ischemia. *Transl Stroke Res* 10:719-728.
- Chen P, Miao Y, Yan P, Wang XJ, Jiang C, Lei Y (2019b) MiR-455-5p ameliorates HG-induced apoptosis, oxidative stress and inflammatory via targeting SOCS3 in retinal pigment epithelial cells. *J Cell Physiol* 234:21915-21924.
- Chien HC, Chan PC, Tu CC, Day YJ, Hung LM, Juan CC, Tian YF, Hsieh PS (2018) Importance of PLC-dependent PI3K/AKT and AMPK signaling in RANTES/CCR5 mediated macrophage chemotaxis. *Chin J Physiol* 61:266-279.
- Clotet B (2007) CCR5 inhibitors: promising yet challenging. *J Infect Dis* 196:178-180.
- Goebel U, Scheid S, Spassov S, Schallner N, Wollborn J, Buerkle H, Ulbrich F (2021) Argon reduces microglial activation and inflammatory cytokine expression in retinal ischemia/reperfusion injury. *Neural Regen Res* 16:192-198.
- He W, Chen S, Chen X, Li S, Chen W (2016) Bioinformatic analysis of potential microRNAs in ischemic stroke. *J Stroke Cerebrovasc Dis* 25:1753-1759.
- Heindl S, Gesierich B, Benakis C, Llovera G, Duering M, Liesz A (2018) Automated morphological analysis of microglia after stroke. *Front Cell Neurosci* 12:106.
- Hu D, Sun S, Wang Y (2020) MicroRNA-455-5p exerts inhibitory effect in cervical carcinoma through targeting S1PR1 and blocking mTOR pathway. *Arch Gynecol Obstet* 301:1307-1315.
- Hu Q, Manaenko A, Bian H, Guo Z, Huang JL, Guo ZN, Yang P, Tang J, Zhang JH (2017) Hyperbaric oxygen reduces infarction volume and hemorrhagic transformation through ATP/NAD(+)/Sirt1 pathway in hyperglycemic middle cerebral artery occlusion rats. *Stroke* 48:1655-1664.
- Hu Y, Yang Z, Bao D, Ni JS, Lou J (2019) miR-455-5p suppresses hepatocellular carcinoma cell growth and invasion via IGF-1R/AKT/GLUT1 pathway by targeting IGF-1R. *Pathol Res Pract* 215:152674.
- Jayaraj RL, Azimullah S, Beiram R, Jalal FY, Rosenberg GA (2019) Neuroinflammation: friend and foe for ischemic stroke. *J Neuroinflammation* 16:142.
- Ji J, Wang J, Yang J, Wang XP, Huang JJ, Xue TF, Sun XL (2019) The intra-nuclear SphK2-S1P axis facilitates M1-to-M2 shift of microglia via suppressing HDAC1-mediated KLF4 deacetylation. *Front Immunol* 10:1241.
- Jin R, Yang G, Li G (2010) Inflammatory mechanisms in ischemic stroke: role of inflammatory cells. *J Leukoc Biol* 87:779-789.
- Jovin DG, Katlaps KG, Ellis BK, Dharmaraj B (2019) Neuroprotection against stroke and encephalopathy after cardiac surgery. *Interv Med Appl Sci* 11:27-37.
- Joy MT, Ben Assayag E, Shabashov-Stone D, Liraz-Zaltsman S, Mazzitelli J, Arenas M, Abduljawad N, Kliper E, Korczyn AD, Thareja NS, Kesner EL, Zhou M, Huang S, Silva TK, Katz N, Bornstein NM, Silva AJ, Shohami E, Carmichael ST (2019) CCR5 is a therapeutic target for recovery after stroke and traumatic brain injury. *Cell* 176:1143-1157.e13.
- Koellhoffer EC, McCullough LD (2013) The effects of estrogen in ischemic stroke. *Transl Stroke Res* 4:390-401.
- Lan YY, Wang YQ, Liu Y (2019) CCR5 silencing reduces inflammatory response, inhibits viability, and promotes apoptosis of synovial cells in rat models of rheumatoid arthritis through the MAPK signaling pathway. *J Cell Physiol* 234:18748-18762.
- Lee Y, Lee SR, Choi SS, Yeo HG, Chang KT, Lee HJ (2014) Therapeutically targeting neuroinflammation and microglia after acute ischemic stroke. *Biomed Res Int* 2014:297241.
- Li P, Wang L, Zhou Y, Gan Y, Zhu W, Xia Y, Jiang X, Watkins S, Vazquez A, Thomson AW, Chen J, Yu W, Hu X (2017) C-C chemokine receptor type 5 (CCR5)-mediated docking of transferred tregs protects against early blood-brain barrier disruption after stroke. *J Am Heart Assoc* 6:e006387.
- Li Z, Rana TM (2014) Therapeutic targeting of microRNAs: current status and future challenges. *Nat Rev Drug Discov* 13:622-638.
- Liu J, Zhang J, Li Y, Wang L, Sui B, Dai D (2016) MiR-455-5p acts as a novel tumor suppressor in gastric cancer by down-regulating RAB18. *Gene* 592:308-315.
- Martin-Blondel G, Brassat D, Bauer J, Lassmann H, Liblau RS (2016) CCR5 blockade for neuroinflammatory diseases—beyond control of HIV. *Nat Rev Neurol* 12:95-105.
- Otxoa-de-Amezaga A, Miró-Mur F, Pedragosa J, Gallizioli M, Justicia C, Gaja-Capdevila N, Ruiz-Jaen F, Salas-Perdomo A, Bosch A, Calvo M, Márquez-Kisinousky L, Denes A, Gunzer M, Planas NM (2019) Microglial cell loss after ischemic stroke favors brain neutrophil accumulation. *Acta Neuropathol* 137:321-341.
- Salameh A, Dhein S, Dähnert I, Klein N (2016) Neuroprotective strategies during cardiac surgery with cardiopulmonary bypass. *Int J Mol Sci* 17:1945.
- Sierksma A, Lu A, Salta E, Vanden Eynden E, Callaerts-Vegh Z, D'Hooge R, Blum D, Buée L, Fiers M, De Strooper B (2018) Deregulation of neuronal miRNAs induced by amyloid- $\beta$  or TAU pathology. *Mol Neurodegener* 13:54.
- Slota JA, Booth SA (2019) MicroRNAs in neuroinflammation: implications in disease pathogenesis, biomarker discovery and therapeutic applications. *Noncoding RNA* 5:35.
- Sorte S, Myburgh R, Krause KH (2011) The chemokine receptor CCR5 in the central nervous system. *Prog Neurobiol* 93:297-311.
- Sorte S, Bonnefont J, Julien S, Marq-Lin N, Rodriguez I, Dubois-Dauphin M, Krause KH (2010) Increased brain damage after ischaemic stroke in mice lacking the chemokine receptor CCR5. *Br J Pharmacol* 160:311-321.
- Strickland IT, Richards L, Holmes FE, Wynick D, Uney JB, Wong LF (2011) Axotomy-induced miR-21 promotes axon growth in adult dorsal root ganglion neurons. *PLoS One* 6:e23423.
- Torabi S, Tamaddon M, Asadolahi M, Shokri G, Tavakoli R, Tasharofi N, Rezaei R, Tavakolpour V, Sazegar H, Kouhkan F (2019) miR-455-5p downregulation promotes inflammation pathways in the relapse phase of relapsing-remitting multiple sclerosis disease. *Immunogenetics* 71:87-95.
- van Kralingen JC, McFall A, Ord ENJ, Coyle TF, Bissett M, McClure JD, McCabe C, Macrae IM, Dawson J, Work LM (2019) Altered extracellular vesicle microRNA expression in ischemic stroke and small vessel disease. *Transl Stroke Res* 10:495-508.
- Vangelista L, Vento S (2017) The expanding therapeutic perspective of CCR5 blockade. *Front Immunol* 8:1981.
- Victoria ECG, de Brito Toscano EC, de Sousa Cardoso AC, da Silva DG, de Miranda AS, da Silva Barcelos L, Sugimoto MA, Sousa LP, de Assis Lima IV, de Oliveira ACP, Brant F, Machado FS, Teixeira MM, Teixeira AL, Rachid MA (2017) Knockdown of C-C chemokine receptor 5 (CCR5) is protective against cerebral ischemia and reperfusion injury. *Curr Neurovasc Res* 14:125-131.
- Wang JJ, Liu F, Yang F, Wang YZ, Qi X, Li Y, Hu Q, Zhu MX, Xu TL (2020a) Disruption of auto-inhibition underlies conformational signaling of ASIC1a to induce neuronal necroptosis. *Nat Commun* 11:475.
- Wang SN, Wang Z, Xu TY, Cheng MH, Li WL, Miao CY (2020b) Cerebral organoids repair ischemic stroke brain injury. *Transl Stroke Res* 11:983-1000.
- Wang Z, Higashikawa K, Yasui H, Kuge Y, Ohno Y, Kihara A, Midori YA, Houkin K, Kawabori M (2020c) FTY720 protects against ischemia-reperfusion injury by preventing the redistribution of tight junction proteins and decreases inflammation in the subacute phase in an experimental stroke model. *Transl Stroke Res* 11:1103-1116.
- Xing Q, Xie H, Zhu B, Sun Z, Huang Y (2019) MiR-455-5p suppresses the progression of prostate cancer by targeting CCR5. *Biomed Res Int* 2019:6394784.
- Xu AL, Zheng GY, Ye HY, Chen XD, Jiang Q (2020) Characterization of astrocytes and microglial cells in the hippocampal CA1 region after transient focal cerebral ischemia in rats treated with Ilexonin A. *Neural Regen Res* 15:78-85.
- Yang B, Singh S, Bressani R, Kanmogne GD (2010) Cross-talk between STAT1 and PI3K/AKT signaling in HIV-1-induced blood-brain barrier dysfunction: role of CCR5 and implications for viral neuropathogenesis. *J Neurosci Res* 88:3090-3101.
- Yao S, Tang B, Li G, Fan R, Cao F (2016) miR-455 inhibits neuronal cell death by targeting TRAF3 in cerebral ischemic stroke. *Neuropsychiatr Dis Treat* 12:3083-3092.
- Zhou Z, Lu J, Liu WW, Manaenko A, Hou X, Mei Q, Huang JL, Tang J, Zhang JH, Yao H, Hu Q (2018) Advances in stroke pharmacology. *Pharmacol Ther* 191:23-42.
- Zuo X, Lu J, Manaenko A, Qi X, Tang J, Mei Q, Xia Y, Hu Q (2019) MicroRNA-132 attenuates cerebral injury by protecting blood-brain-barrier in MCAO mice. *Exp Neurol* 316:12-19.

P-Reviewer: Espinosa-Garcia C; C-Editor: Zhao M; S-Editors: Yu J, Li CH; L-Editors: Yu J, Song LP; T-Editor: Jia Y

Experiment 1, animal study.



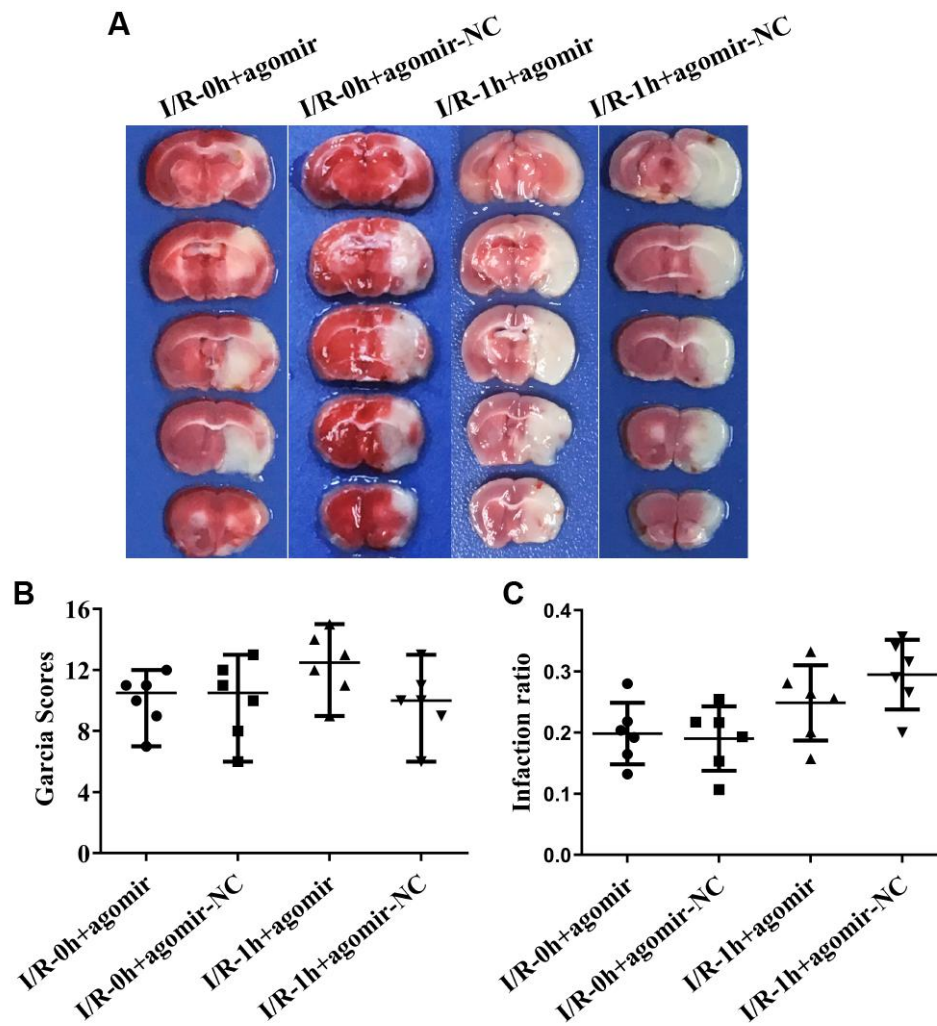
Experiment 2, in vitro study.



**Additional Figure 1 Experimental design, animal groups classification and timeline.**

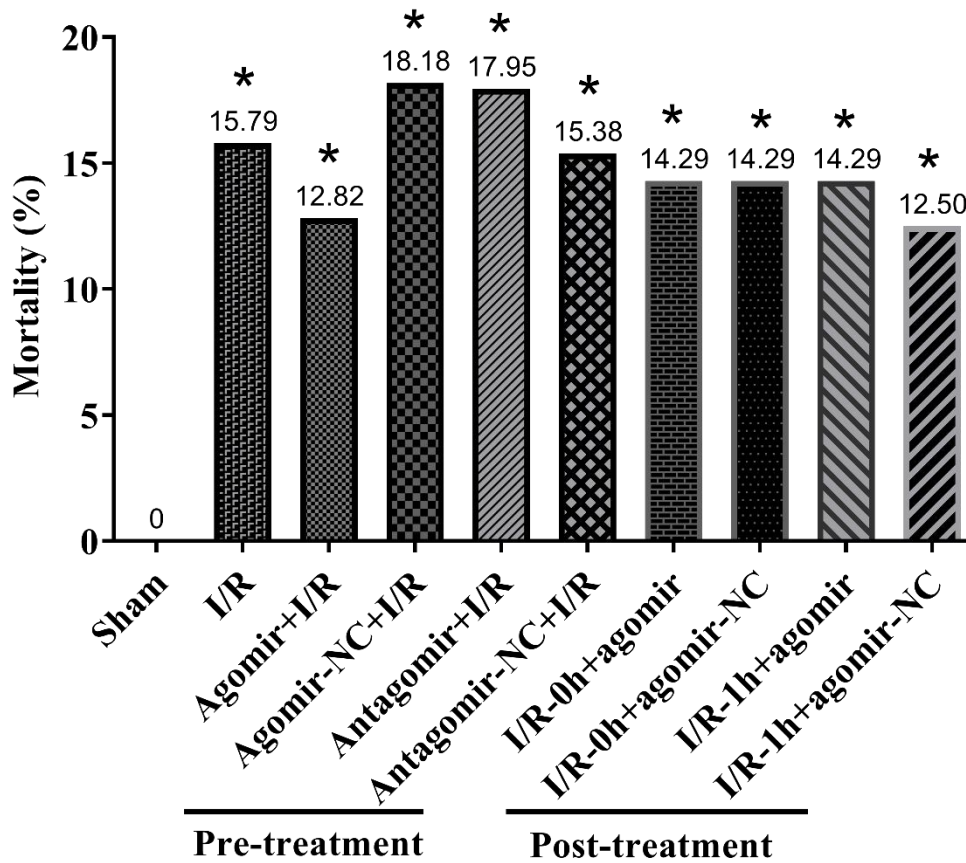
i.c.v: Intracerebroventricular injection; I/R: ischemia/reperfusion; IF: immunofluorescence; MCAO: middle cerebral artery occlusion; NC: negative control; OGD: oxygen–glucose deprivation; PCR: polymerase chain reaction; WB: western blot.





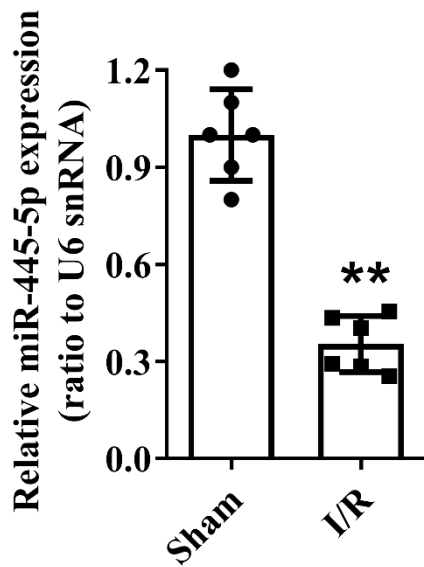
**Additional Figure 2 Administration of agomiR-455-5p at 0 and 1 hour after reperfusion has no protective effect on infarct volume and neurological deficits.**

(A) Representative 2,3,5-triphenyltetrazolium hydrochloride-stained brain slices in agomiR-455-5p or its negative control post-treated (0 hour and 1 hour after reperfusion) mice. (B) Quantitative results of infarction ratio. (C) Garcia scores at 24 hours after I/R. Data are presented as mean  $\pm$  SD ( $n = 6$  per group). Data in Garcia scores were analyzed by non-parametric Kruskal-Wallis rank sum test and data in infarction ratio were analyzed by one-way analysis of variance followed by Tukey's post hoc test. I/R: Ischemia/reperfusion; NC: negative control.



**Additional Figure 3** The mortality of mice in the study.

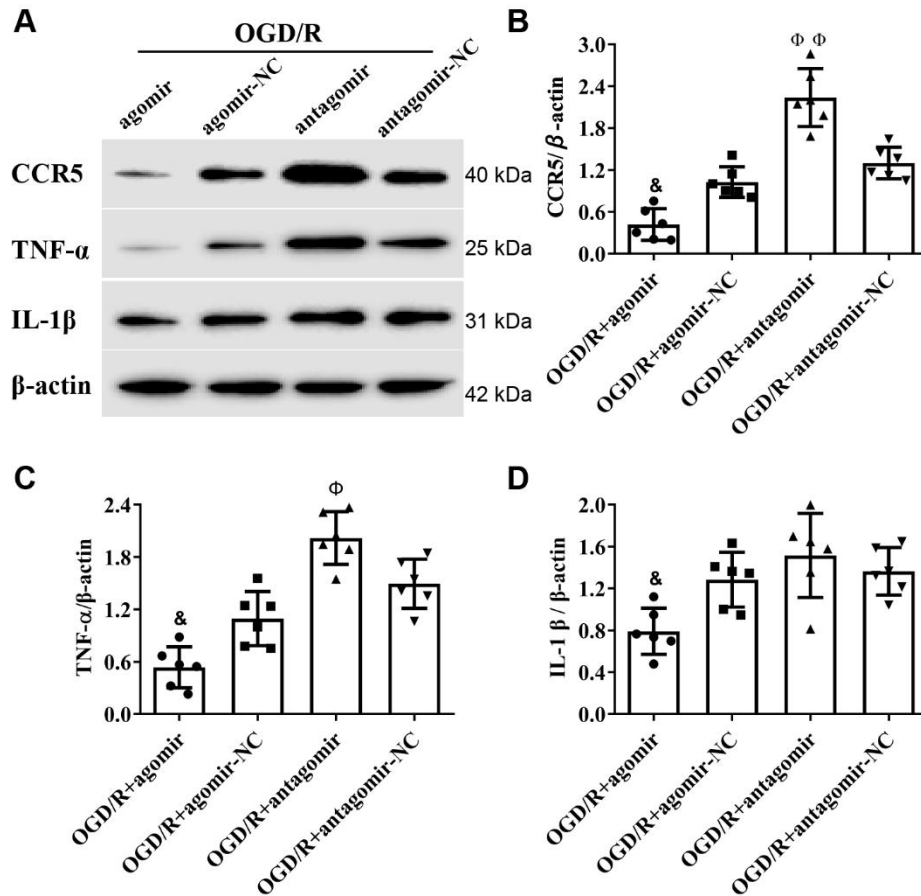
In the treatment groups, agomir-455-5p, antagomir-455-5p, and their negative controls (agomir-NC and antagomir-NC) were injected intracerebroventricularly 2 hours before or 0 and 1 hour after MCAO in mice. Neither pre-treatment or post-treatment with agomir-455-5p affected the mortality after I/R. Data are presented as number. \* $P < 0.05$ , vs. sham group (Fisher exact test). I/R: Ischemia/reperfusion; NC: negative control.



**Additional Figure 4 I/R reduces the level of miR-455-5p in the peripheral blood in cerebral I/R mice.**

The expression of miR-455-5p in the peripheral blood decreased at 24 hours after I/R. Data are presented as mean  $\pm$  SD ( $n = 6$ ). \* $P < 0.05$ , vs. I/R group (Student's t-test). I/R: Ischemia/reperfusion; snRNA: small nuclear RNA.





**Additional Figure 5 AgomiR-455-5p inhibits the expression of CCR5 and pro-inflammatory factors TNF- $\alpha$  and IL-1 $\beta$  24 hours after OGD/R, and antagomiR-455-5p reverses the effects.**

(A) Representative western blot bands of CCR5, TNF- $\alpha$  and IL-1 $\beta$  in microglia after OGD/R with /without agomiR-455-5p or antagomiR-455-5p treatment. (B-D) Quantitative results of CCR5, TNF- $\alpha$ , and IL-1 $\beta$  production. Data are presented as mean  $\pm$  SD ( $n = 6$ ). & $P < 0.05$ , vs. OGD/R + agomir-NC group;  $\phi P < 0.05$ , vs. OGD/R + antagomir-NC group (one-way analysis of variance followed by Tukey's post hoc test). CCR5: C-C chemokine receptor type 5; IL-1 $\beta$ : interleukin-1 $\beta$ ; NC: negative control; OGD/R: xygen-glucose deprivation/reoxygenation; TNF- $\alpha$ : tumor necrosis factor alpha.

**Additional Table 1 Animal assignment in each group**

Groups	Infarct volume,			Brain water			Total
	Garcia score	Foot fault, beam walking	Evans blue content	content	WB, PCR	Immunofluorescence	
Pre-treatment							
Sham	0/0/6	0/0/6	0/0/6	0/0/6	0/0/6	0/0/3	33
I/R	1/1/6	2/0/6	2/0/6	1/0/6	0/1/6		38
Agomir+I/R	2/0/6	1/1/6	1/0/6	1/0/6	0/0/6	0/0/3	44
Agomir-NC+I/R	2/1/6	2/0/6	1/1/6	1/1/6	1/0/6	1/0/3	39
Antagomir+I/R	3/0/6	1/1/6	2/1/6	1/0/6	0/0/6		39
Antagomir-NC+I/R	2/0/6	1/1/6	1/0/6	1/1/6	1/1/6		39
Post-treatment							
I/R-0h+agomir	1/0/6						7
I/R-0h+agomir-NC	1/0/6						7
I/R-1h+agomir	1/0/6						7
I/R-1h+agomir-NC	1/1/6						8
Total	77	46	45	43	40	10	261

Data are expressed as died/excluded/survived. I/R: Ischemia/reperfusion; NC: negative control; PCR: polymerase chain reaction; WB: western blot.